AFCRL-67-0494

Contract Nr. 61(052)-902

20 June 1967

SCIENTIFIC REPORT NO. 4

DETERMINATION OF THE MEAN VALUES OF CONDUCTIVITY AND DIELECTRIC CONSTANT FROM THE FIELD STRUCTURE OF A MAGNETIC DIPOLE.

October 1966 - June 1967

Dr. W. BITTERLICH

VLF PROJECT

INNSBRUCK, AUSTRIA

THIS RESEARCH HAS BEEN SPONSORED IN PART BY THE UNITED STATES GOVERNMENT UNDER CONTRACT 61(052)-902.

PREFACE

The present report is part of a thesis by Walter KELLNER, collaborator of the VLF Project Innsbruck.

Contractor: Dr. Wolfram BITTERLICH
Kaiser-Franz-Josefstr. 5
A-6020 Innsbruck, Austria.

ABSTRACT

The equations for a magnetic dipole in a homogeneous, conductive medium are analyzed. The field is shown to be elliptically polarized in the transition zone between near field and far field. Quantities are introduced which are easy to determine by experiment: from them, the complex propagation constant can be determined at a given distance. Thus, conductivity and dielectric constant can be calculated for a given frequency. The applicability of this method is confined to the region of validity of the basic expressions. This comprises the condition that the cavity which contains transmitter and receiver is small as compared to the wave-length in matter. Our measurements at 120 kc/sec satisfied this condition.

The principle of measurement and its evaluation are described. The results are compared with results obtained from natural rock samples.

TABLE OF CONTENTS

DETERMINATION OF THE MEAN VALUES OF CONDUCTIVITY AND DIELECTRIC CONSTANT FROM THE FIELD STRUCTURE OF A MAGNETIC DIPOLE

1. THEORY

1.1. Fundamental equations

The radiation of a magnetic dipole is considered under the following assumptions:

1. The medium is homogeneous, isotropic and unbounded. The decisive rock parameters ε, μ and σ are actually constant.
2. Transmitter and receiver are embedded in this medium.
3. The distance r between transmitter and receiver is so large that both, transmitter and receiver, may be considered as point-shaped.

Then the measured magnetic field strength components in complex form read as follows : [1], [2], [9]

$$H_r^* = \frac{m}{2\pi} \cos\vartheta \, \frac{e^{i(\omega t - kr)}}{r} \left[\frac{ik}{r} + \frac{1}{r^2}\right] \qquad (1)$$

$$H_\vartheta^* = \frac{m}{4\pi} \sin\vartheta \, \frac{e^{i(\omega t - kr)}}{r} \left[-k^2 + \frac{ik}{r} + \frac{1}{r^2}\right] \qquad (2)$$

m = n.I.F = dipole moment
n.F = number of turns by the area of the transmitting antenna
I = current intensity,
r = transmitter - receiver distance
ϑ = angle between the dipole axis and radius vector to the point of measurement,
k = complex propagation constant for which the following expressions are valid:

$$k^2 = \omega^2 \varepsilon \varepsilon_o \mu \mu_o - i\sigma\omega\mu\mu_o = (k_1 - ik_2)^2 \qquad (3)$$

$$k_1 = \mathrm{Re}\, k = \sqrt{\frac{1}{2}\, \omega^2 \varepsilon \varepsilon_o \mu_o \mu \left(1 + \sqrt{1 + \left(\frac{\sigma}{\omega \varepsilon \varepsilon_o}\right)^2}\right)} \qquad (4)$$

$$k_2 = -\mathrm{Im}\, k = \sqrt{\frac{1}{2}\omega^2 \varepsilon \varepsilon_0 \mu_0 \mu \left(-1 + \sqrt{1 + \left(\frac{\sigma}{\omega \varepsilon \varepsilon_0}\right)^2}\right)}. \qquad (5)$$

As k^2 lies in the fourth quadrant of the Gaussian plane, the values for k lie always in the hatched part. The following relation is valid:

$$k_2 \leq k_1 \qquad (6)$$

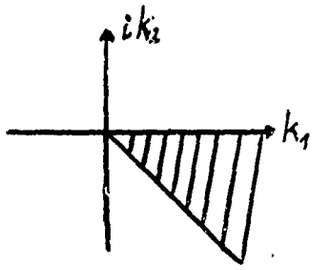

1.2 Determination of σ and ε:

If k_1 and k_2 can be measured, σ and ε may be determined at a given frequency and at $\mu = 1$ (valid for the majority of rocks). From (3) it follows that:

$$\mathrm{Re}\, k^2 = k_1^2 - k_2^2 = \omega^2 \varepsilon \varepsilon_0 \mu_0$$

$$\mathrm{Im}\, k^2 = -2k_1 k_2 = -\sigma \omega \mu_0$$

and furthermore

$$\varepsilon = \frac{k_1^2 - k_2^2}{\varepsilon_0 \mu_0 \omega^2} = \frac{9 \cdot 10^{16}}{4\pi^2} \frac{k_1^2 - k_2^2}{\gamma^2} = 2.285 \cdot 10^{15} \frac{k_1^2 - k_2^2}{\gamma^2} \qquad (7)$$

$$\sigma = \frac{2k_1 k_2}{\mu_0 \omega} = \frac{10^7}{4\pi^2} \frac{k_1 k_2}{\gamma} = 2.535 \cdot 10^5 \frac{k_1 \cdot k_2}{\gamma} \qquad (8)$$

1.3 Polarization ellipse [1]

For the far field ($k_1 r \gg 1$) of a dipole, all terms of an order higher than $1/r$ may be neglected in Eq. (1) and (2). Only a magnetic component and an electric componenet are left over which in accordance with Sommerfeld's radiation condition behave like spherical waves. Under these assumptions, the paper quoted under [4] gives among other things also a method of determining the attenuation factor k_2.

If this approximation is not valid, the main field is polarized elliptically (main field is the electric field of an electrical dipole, and the magnetic field of a magnetic dipole). In (1) and (2), theory yields complex expressions for H_r and H_ϑ which are interpreted as follows:

Let us turn from the time dependence $\exp(i\omega t)$ to real trigonometric functions, we thus obtain the real field strength components H_r and H_ϑ:

$$H_r = A \cos(\omega t - k_1 r + \delta_1) \qquad (1a)$$

$$H_\vartheta = B \cos(\omega t - k_1 r + \delta_2) \qquad (2a)$$

δ_1 and δ_2 are the phase angles of the complex numbers in brackets of Eqs. (1) and (2).

The maximum values of the oscillation A and B are calculated as absolute values of (1) and (2)

$$A = |H_r^*|$$
$$B = |H_\vartheta^*| .$$

Snap-shots of the field taken at a certain moment yield the well-known pictures of Hertzian lines of force [5]. The resulting field strength is formed in accordance with the rules of vector addition.

(1a) and (2a) also show the influence of the phase constants δ_1 and δ_2 on the amount and direction of field strength.

Such snap-shots cannot be made by experiment.

The observer has the possibility of taking the position at a certain point of the coordinates (r, ϑ) and of measuring the time mean values of received field strength (amount and direction).

From (1a) and (2a) it can be seen that the phases of the two oscillations in the directions r and ϑ are shifted by

$$\delta = \delta_2 - \delta_1 . \qquad (9)$$

For r = const, (1a) and (2a) may be written as follows, with the phase constants $k_1 r$, δ_1 and δ_2 being omitted:

$$H_r = A \cos \omega t \qquad (1b)$$

$$H_\vartheta = B \cos (\omega t + \delta). \qquad (2b)$$

The observer thus measures an elliptically polarized field.

Fig. 1 shows the formation of the rotating field ellipse from the field strength components H_r and H_ϑ. The angle ψ is counted counterclockwise from the radius vecotr toward maximum received field strength. The small axis of the ellipse is H_2.

δ is calculated at a later time, yet the definition of δ_1 and δ_2 shows δ being a function of k_1, k_2 and r(cf. (1a) and (2a)). Since δ in Section 1.8 is shown to be measured, there exists the possibility of

1.4 <u>determining k_1 and k_2</u>

Measuring $\delta = \delta(k_1, k_2, r)$ and r alone does not yield k_1 and k_2. We need another quantity which also depends on k_1, k_2 and r and which is just as easy to measure.

Polarisation ellipse and measurement of the angles

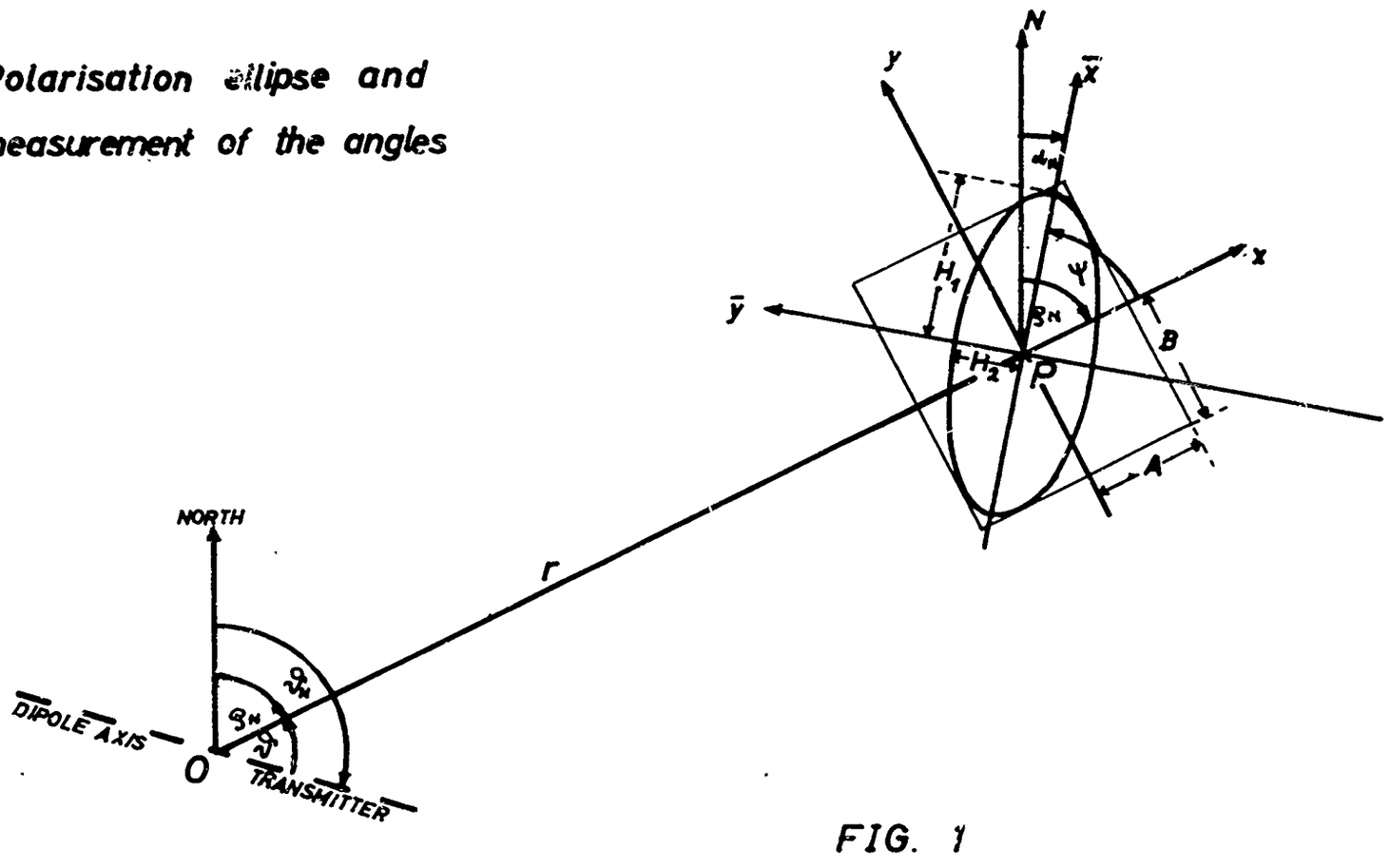

FIG. 1

These conditions are fulfilled by the function [3], [5]

$$G = \frac{H_o}{H_{90}} = \frac{|H_r^*|/\cos\delta}{|H_\delta^*|/\sin\delta} = \frac{A}{B} \tan\delta \qquad (10)$$

which in the course of VLF work has frequently been examined, H_0 and H_{90} being the field strengths at 0° and 90°, respectively.

The following section proves that G and δ may be written as follows:

$$\delta = \delta(k_1 r, k_2 r)$$

$$G = G(k_1 r, k_2 r) .$$

Hence it is quite sufficient to solve the above system of equations for $k_1 r$ and $k_2 r$, the resulting values being divided by r. Thus, k_1 and k_2 are obtained.

1.5 Calculation of G and δ

Substituting $k = k_1 - ik_2$ in (1) and (2) we obtain:

$$H_r^* = \frac{m}{2\pi} \cos\delta \frac{e^{i(\omega t - k_1 r)}}{r} e^{-k_2 r} \left[\frac{1}{r^2} + \frac{k_2}{r} + \frac{ik_1}{r}\right] \qquad (1c)$$

$$H_\delta^* = \frac{m}{4\pi} \sin\delta \frac{e^{i(\omega t - k_1 r)}}{r} e^{-k_2 r} \left[-k_1^2 + k_2^2 + \frac{k_2}{r} + \frac{1}{r^2} + 2ik_1 k_2 + \frac{ik_1}{r}\right] \qquad (2c)$$

For the purpose of abbreviation, we substitute the following expressions for the real part and imaginary part in parentheses:

$$\frac{k_2}{r} + \frac{1}{r^2} = a_1 \qquad \frac{k_1}{r} = b_1$$

$$-k_1^2 + k_2^2 + \frac{k_2}{r} + \frac{1}{r^2} = a_2 \qquad 2k_1 k_2 + \frac{k_1}{r} = b_2$$

Thus,

$$\tan \delta_1 = \frac{b_1}{a_1}$$

$$\tan \delta_2 = \frac{b_2}{a_2}$$

with δ_1 and δ_2 being phase constants which in (1c) and (2c) may be counted among the terms exp $i(\omega t - k_1 r)$, yielding:

$$H_r \sim \cos (\omega t - k_1 r + \delta_1)$$

$$H_i \sim \cos (\omega t - k_1 r + \delta_2).$$

With $\delta = \delta_2 - \delta_1$ it follows that

$$\tan \delta = \frac{\tan \delta_2 - \tan \delta_1}{1 + \tan \delta_1 \tan \delta_2} = \frac{a_1 b_2 - a_2 b_1}{a_1 a_2 + b_1 b_2} .$$

For G we obtain

$$G = \frac{A/\cos \delta}{B/\sin \delta} = 2 \sqrt{\frac{a_1^2 + b_1^2}{a_2^2 + b_2^2}} .$$

Substituting the above values for a_1, b_1, a_2, b_2, we obtain after brief calculation

$$\tan \delta = \frac{k_1 r \left[2k_1 r + (k_1 r)^2 + (k_2 r)^2\right]}{1 + 2k_2 r + 2(k_2 r)^2 + k_2 r \left[(k_1 r)^2 + (k_2 r)^2\right]} \qquad (11)$$

$$G = 2 \sqrt{\frac{(1 + k_2 r)^2 + (k_1 r)^2}{1+2k_2 r+3(k_2 r)^2-(k_1 r)^2+2k_2 r \left[(k_1 r)^2+(k_2 r)^2\right] + \left[(k_1 r)^2+(k_2 r)^2\right]^2}} \qquad (12)$$

Hence, G and δ really depend only on $k_1 r$ and $k_2 r$, as stated in Section 1.4.

1.6. Discussion

The functions (11) and (12) were computed on the ZUSE Z23V computor of the Institut für Rechentechnik, University of Innsbruck.

The results are given in Figs. 2 and 3. They show the functions G and δ as dependent on

$$x = k_1 r \quad . \tag{13}$$

Because of (6) it seemed favorable not to choose $k_2 r$ as parameter, but to express $k_2 r$ in percents of $k_1 r$, thus putting

$$k_2 r = p k_1 r \ .$$

$$p = \frac{k_2}{k_1} \ [\%] \tag{14}$$

is the parameter chosen in the family of curves.

The physical importance of x and p is explained as follows:

x is the distance related to the wave-length of radiation in matter multiplied by 2π.

p depends only on the ratio charge carrier motion : displacement current = $\sigma : \omega \varepsilon \varepsilon_0$, as can be seen from (4) and (5).

$$p = \frac{\sqrt{1 + \left(\frac{\sigma}{\omega \varepsilon \varepsilon_0}\right)^2} - 1}{\frac{\sigma}{\omega \varepsilon \varepsilon_0}} \tag{15}$$

For $\frac{\sigma}{\omega \varepsilon \varepsilon_0} < 0.2$

$$p \doteq \frac{1}{2} \frac{\sigma}{\omega \varepsilon \varepsilon_0} \tag{16}$$

is valid with good approximation (slide rule accuracy), for $\frac{\sigma}{\omega \varepsilon \varepsilon_0} > 10$ we may write

$$p \doteq 1 - \frac{\omega \varepsilon \varepsilon_0}{\sigma} \quad . \tag{17}$$

The intermediate region not covered by the approximation expressions is represented in Fig. 4.

From (16) and (17) it can be seen that the curves in Figs. 2 and 3 with p = 0 illustrate the conditions of an ideal insulator, whereas p = 100 corresponds to an ideal conductor.

1.7. Relation between G, δ and the field structure

In the near field ($r \ll \lambda$), the field has the structure of an ordinary magnetic dipole. In the expressions (1) and (2), only the terms $\sim 1/r^3$ are decisive which correspond to Bio-Savart's law in the stationary case. For small values of $k_1 r$, all curves of $G(x,p)$ and $\delta(x,p)$ converge. Here the field structure is independent of whether we have a conductor or an insulator. In practice, the near field can be determined as follows:

$$k_1 r \leqslant 0.1 \quad . \tag{18}$$

This means that for distances $\leqslant 0.016$ timer the wavelength, the displacement current in any case may be ngelected. The values for G and δ in this region are

$$G = 2$$
$$\delta \leqslant 1^{\circ}.$$

Hence, the phase difference is negligibly small, the field being linearly polarized. At a fixed point of measurement,

$$\vec{H}^2 = |H_r|^2 + |H_\vartheta|^2 .$$

In the far field ($r \gg \lambda$), the curves for G fuse together, whereas the phase difference approaches a boundary value. From (11) we obtain

$$\lim_{r \to \infty} \tan \delta = \frac{k_1}{k_2} = \frac{1}{p} \quad . \tag{19}$$

Let us take

$$k_1 r \geqslant 10$$

as a definition of the far field and let us make an accurate examination.

The phase difference then differs from the boundary value (19)

FIG. 2 : Phase shift delta vs. $x = k_1 r$, parameter $p = k_2/k_1$ (%)

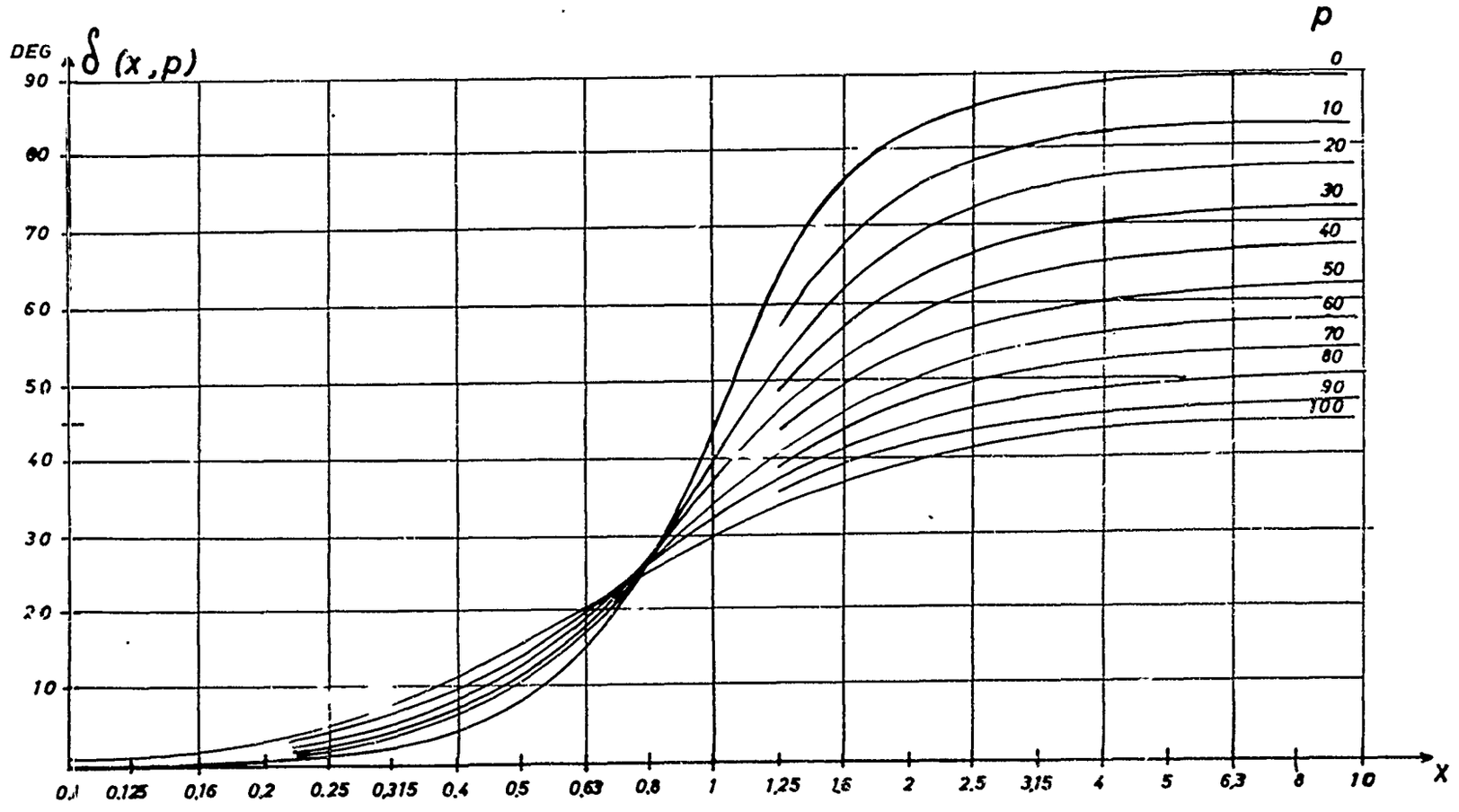

FIG. 3: G vs. $x = k_1 r$, parameter $p = k_2/k_1$ (%)

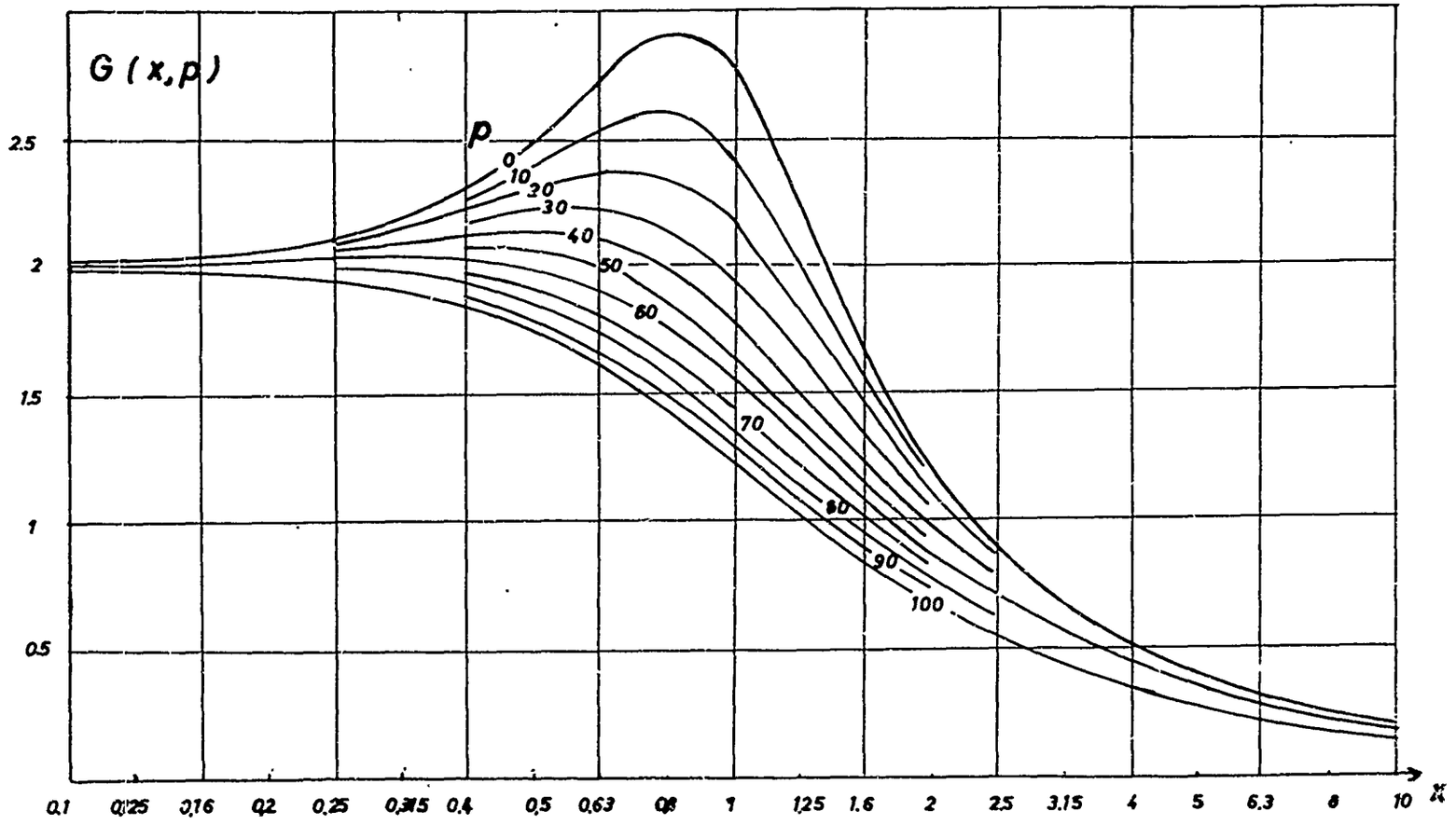

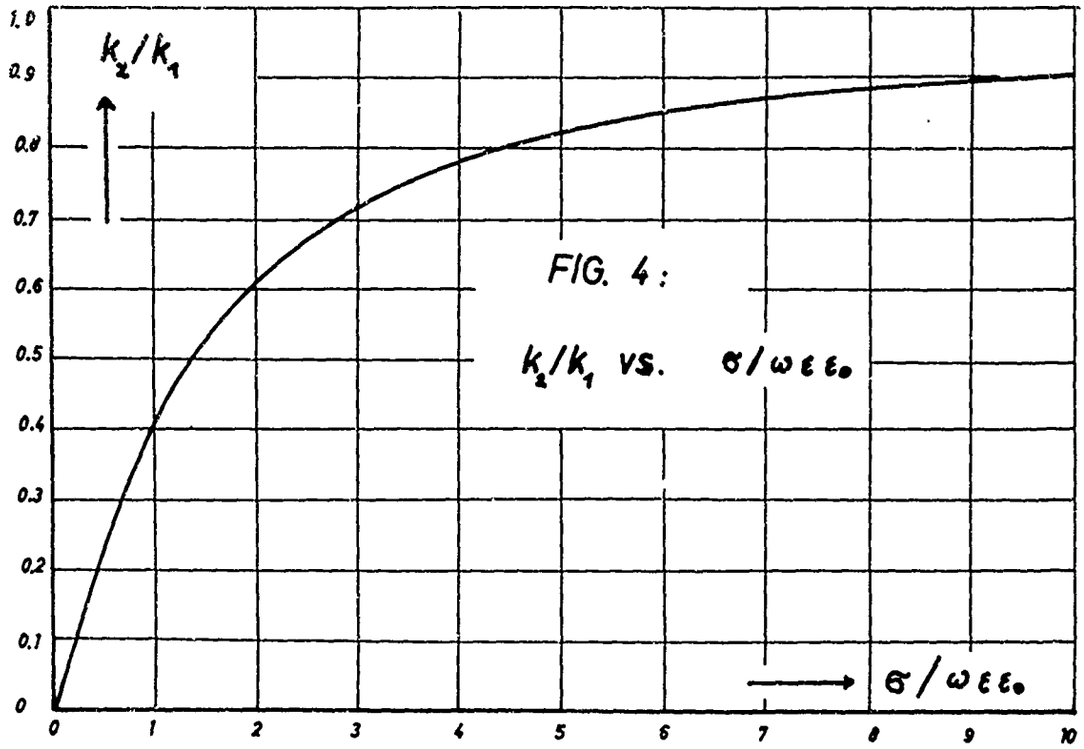

FIG. 4:

k_2/k_1 vs. $\sigma/\omega\varepsilon\varepsilon_0$

FIG. 5:

Far Field Diagram

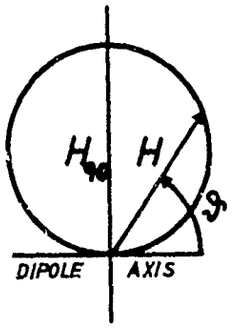

$H = H_{90} \sin \vartheta$

FIG. 6:

Pedal Locus Curve

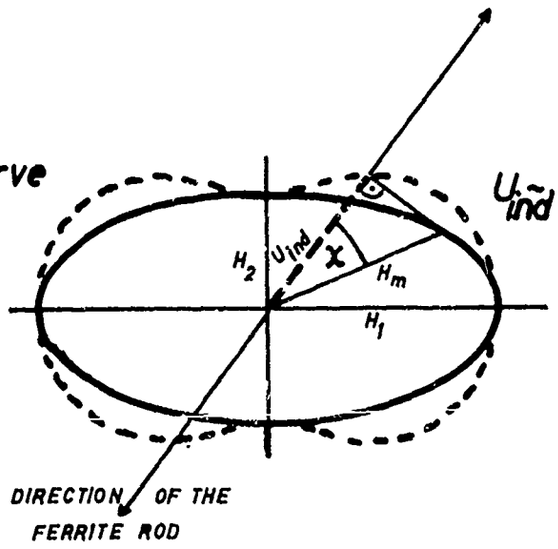

$U_{ind} \sim H_m \cos\chi$

by no more than 0.3°. G is smaller than 0.2. This does not mean that elliptic polarization here could be neglected.

For an angle of ϑ for which we have

$$\tan \vartheta = G ,$$

$|H_r^*| = |H_\vartheta^*|$ is valid as can be seen from (10).

For this angle, a distinct rotating field ellipse may be expected. Substituting $k_1 r = 10$ in the above equation, we obtain

$$8^\circ \leqslant \vartheta \leqslant 11.3^\circ .$$

The statement that a dipole does not radiate in the direction of its oscillation is not exactly valid, it follows from the consideration of H_ϑ only.

Field strength diagrams therefore do not attain the value zero for any value of ϑ, as can be seen in Fig. 5, since H_r always prevails for a small angle ϑ.

We are now going to prove in how far the far field diagram of Fig. 5 is valid for $k_1 r = 10$.

If the component H_ϑ is approximately 10 times H_r, we may consider the wave to be linearly polarized: with

$$0.14 < G < 0.2 \quad \text{(Fig. 3)}$$

we then obtain

$$54^\circ < \vartheta < 64^\circ$$

according to (10).

This means that the far field diagram of Fig. 5 is valid only from an angle of approximately 60° onward. Hence, $k_1 r = 10$ is not a useful limit.

As the concept of far field can be outlined only with a certain arbitrariness, and a clear definition of concepts being desirable, the following suggestion shall be made:

We may speak of a far field in those cases where the wave may be looked upon as being linearly polarized from an angle of $\vartheta \geq 10^{\circ}$, in spite of a phase difference between H_r and H_ϑ.

Under the following condition the wave may furthermore with good approximation be assumed to be linearly polarized:

$$H_\vartheta \geq 10 \cdot H_r \,.$$

Because of (10) it thus follows that

$$G < 0.18$$

which according to (12) means that

$$k_1 r > 100 \,. \tag{20}$$

Summary:

The near field corresponds to the field of a stationary dipole. We speak of a near field when

$$k_1 r \leq 0.1. \tag{18}$$

The defintion of far field is based on the assumption that the typical far field diagram $|H| \sim \sin \vartheta$ is valid and that H_r at an angle of $\vartheta = 10^{\circ}$ is 1/10 of H_ϑ. This yielded

$$k_1 r > 100.$$

The near field - far field transition zone in which the H field is elliptically polarized lies in the region of

$$0.1 < k_1 r \leq 100 \,,$$

where differences between σ and ε have maximum influence on the field structure. From the above structure characterized by G and δ, conclusions as to σ and ε may be made by evaluating the re-

sulting polarization ellipse.

1.8 Determination of G and δ from the polarization ellipse

If there exists an elliptically polarized field, a voltage proportional to the diameter of the ellipse in the direction of the receiving antenna is induced in the receiving antenna which behaves like a magnetic dipole (ferrite rod). When turning the receiving antenna through 360°, voltages are measured which are not proportional to the rotating field ellipse, but which have values that lie on a pedal locus curve of the ellipse with respect to the point of revoluation P (cf. Fig. 6). This has already been described in [5]. Ellipse and pedal locus curve contact each other in the peak values so that the voltages induced in these directions are proportional to the field strengths H_1 and H_2 of Fig. 1 . Thus we have

$$U_1 \sim H_1$$
$$U_2 \sim H_2 .$$

It is shown hereinafter that it is quite sufficient to measure the axial ratio of the rotating field ellipse

$$v = \frac{H_1}{H_2} = \frac{U_1}{U_2} \qquad (21)$$

and the angle ψ between the radius vector and the maximum field strength. G and δ can then be determined.

For this purpose, we place a Cartesian coordinate system (x,y) through the point P so that the x-axis coincides with the radial direction.

In Eqs. (1b) and (2b) we substitute

$$x \text{ for } H_r$$
$$y \text{ for } H_\varphi ,$$

writing

$$x = A \cos \omega t$$
$$y = B \cos (\omega t + \delta) .$$

Elimination of t yields the equation of the rotating field ellipse, i.e., the path described by the tip of $\vec{H}$ around the point P:

$$\left(\frac{x}{A \sin\delta}\right)^2 + \left(\frac{y}{B \sin\delta}\right)^2 - \frac{2xy \cos\delta}{AB \sin^2\delta} = 1 . \qquad (22)$$

The system $(\bar{x},\bar{y})$ is placed so that the ellipse here has standard shape:

$$\left(\frac{\bar{x}}{H_1}\right)^2 + \left(\frac{\bar{y}}{H_2}\right)^2 = 1 . \qquad (23)$$

The system $(\bar{x},\bar{y})$ is displaced with respect to (x,y) by the angle of ψ. There exists the following relation:

$$\bar{x} = x \cos\psi + y \sin\psi$$
$$\bar{y} = -x \sin\psi + y \cos\psi .$$

Substituting this relation in (23) we obtain:

$$\frac{x^2}{\frac{H_1^2 \cdot H_2^2}{H_2^2\cos^2\psi + H_1^2 \sin^2\psi}} + \frac{y^2}{\frac{H_1^2 \cdot H_2^2}{H_2^2 \sin^2\psi + H_1^2\cos^2\psi}} - \frac{2xy}{\frac{H_1^2 H_2^2}{(H_1^2 - H_2^2)\frac{1}{2} \sin 2\psi}} = 1 .$$

Comparison of coefficients with (22) yields:

$$A^2 \sin^2\delta = \frac{H_1^2 H_2^2}{H_2^2\cos^2\psi + H_1^2\sin^2\psi} \qquad (24)$$

$$B^2 \sin^2\delta = \frac{H_1^2 H_2^2}{H_1^2\cos^2\psi + H_2^2\sin^2\psi} \qquad (25)$$

$$AB \frac{\sin^2\delta}{\cos\delta} = \frac{H_1^2 H_2^2}{(H_1^2 - H_2^2)\frac{1}{2} \sin^2\psi} . \qquad (26)$$

Dividing (24) by (25) we obtain

$$w = \frac{A}{B} = \sqrt{\frac{H_1^2\cos^2\Psi + H_2^2\sin^2\Psi}{H_2^2\cos^2\Psi + H_1^2\sin^2\Psi}} \cdot \sqrt{\frac{v^2\cos^2\Psi + \sin^2\Psi}{v^2\sin^2\Psi + \cos^2\Psi}} \qquad (27)$$

where (21) has been substituted. The root of the product of (24) and (25) yields the left-hand side of (26) except for the factor of $1/\cos\delta$.

$$\left\{ \frac{H_1^4\, H_2^4}{(H_2^2\cos^2\Psi + H_1^2\sin^2\Psi)(H_1^2\cos^2\Psi + H_2^2\sin^2\Psi)} \right\}^{1/2} \frac{1}{\cos\delta} = \frac{H_1^2 H_2^2}{(H_1^2 - H_2^2)\frac{1}{2}\sin 2\Psi}$$

After an easy transformation we obtain

$$\cos\delta = \frac{(v^2 - 1)\sin 2\Psi}{\sqrt{\left[(v^2 - 1)\sin^2\Psi\right]^2 + 4v^2}} \quad , \qquad (28)$$

The expressions (27) and (28) yield the following statements:

If the axial ratio v of the polarization ellipse and the angle of rotation Ψ are given, the phase difference δ and the ratio of the maximum values of the field strength component $w = \frac{A}{B}$ can be determined.

If, however, $\frac{A}{B}$ is given, G follows from (10):

$$G = \frac{A}{B} \tan \delta .$$

For the purpose of facilitating the evaluation of measurement, the expressions (27) and (28) were computed on a ZUSE Z23V computor (Institut für Rechentechnik) for a series of v and Ψ values. w and δ are illustrated in Figs. 7 and 8 as functions of v, with Ψ being the parameter.

1.9. Evaluation scheme

Let us first continue the statements of section 1.4:

Solving the system

$$G = G(x,p)$$
$$\delta = \delta(x,p)$$

for x and p by means of Figs. 2 and 3 is quite troublesome.

For this reason, both figures were combined in Fig. 9 where G and δ are plotted on the coordinate axes, p having fixed values along the plotted curves and x having fixed values along the dashed curves. Exactly one pair of values, x and p, can be read from this figure for the pair of values G and δ. As the intervals for x and p are chosen small, linear interpolation is possible. Deviation of x and p may easily be read off at given deviation of G and δ.

k_1 and k_2 follow from x and p according to Eq. (13) and (14):

$$k_1 = \frac{x}{r} \qquad (13a)$$

$$k_2 = p\frac{x}{r} . \qquad (14a)$$

Substituting these expressions in (7) and (8) we obtain the final expressions

$$\varepsilon = 2.285 \cdot 10^{15} \frac{x^2(1-p^2)}{r^2\gamma^2} \quad [-] \qquad (7a)$$

$$\sigma = 2.535 \cdot 10^5 \left(\frac{x}{r}\right)^2 \frac{p}{\gamma} \quad \left[\Omega^{-1}m^{-1}\right] . \qquad (8a)$$

The steps of evaluation are illustrated by the following diagram:

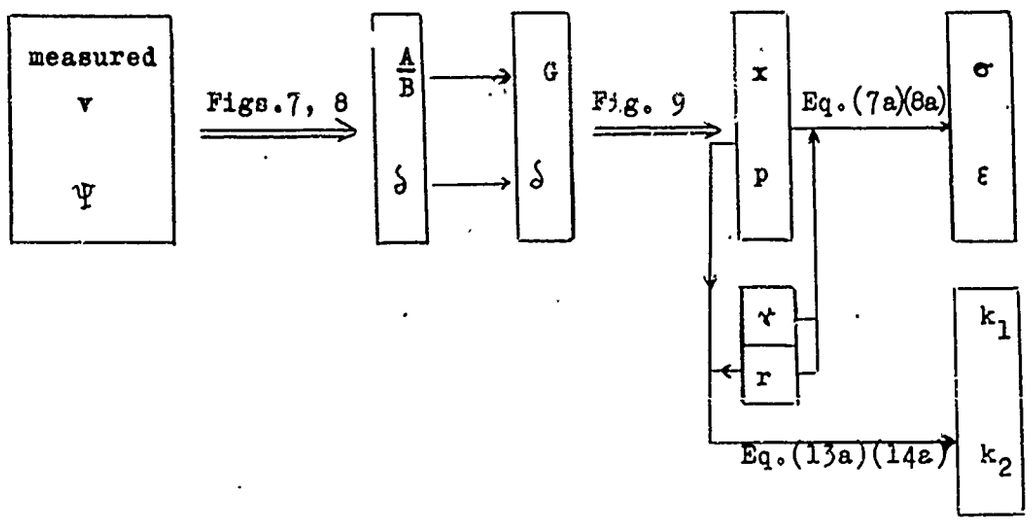

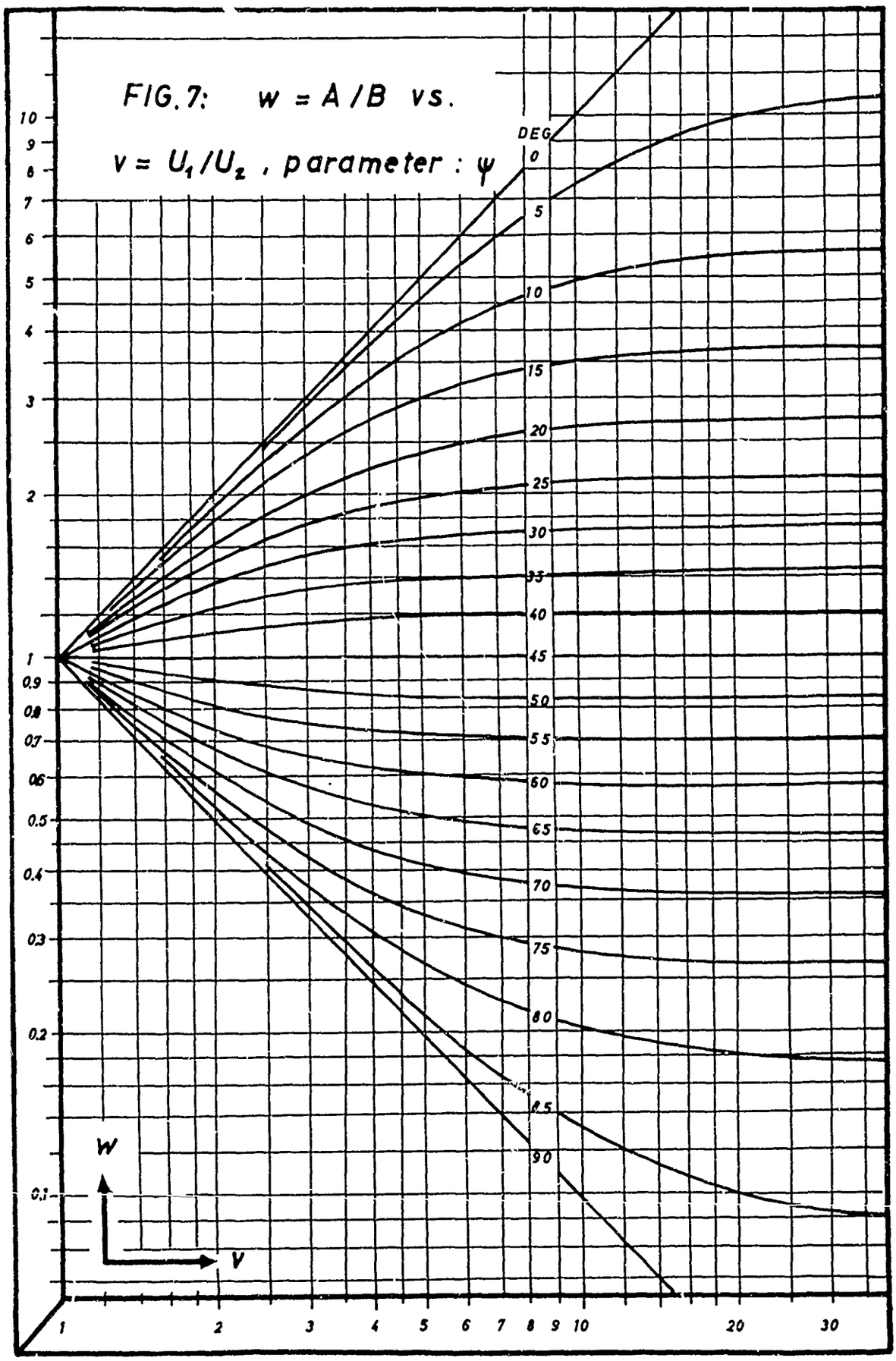
FIG. 7: w = A/B vs.
v = U1/U2 , parameter : ψ
DEG
0
5
10
15
20
25
30
35
40
45
50
55
60
65
70
75
80
85
90
10
9
8
7
6
5
4
3
2
1
0.9
0.8
0.7
0.6
0.5
0.4
0.3
0.2
0.1
W
V
1
2
3
4
5
6
7
8
9
10
20
30

FIG . 8: δ vs . v . parameter : ψ

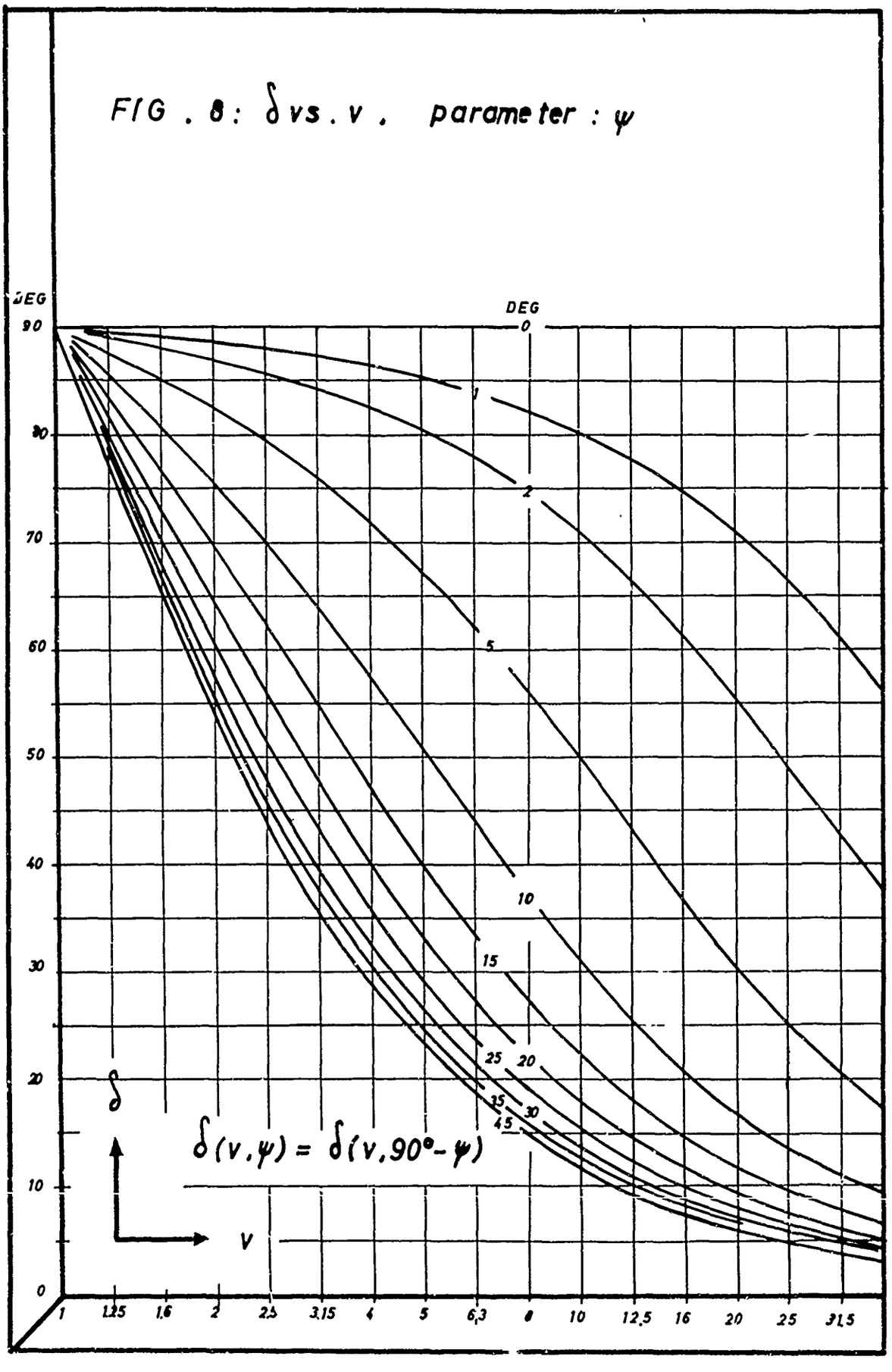

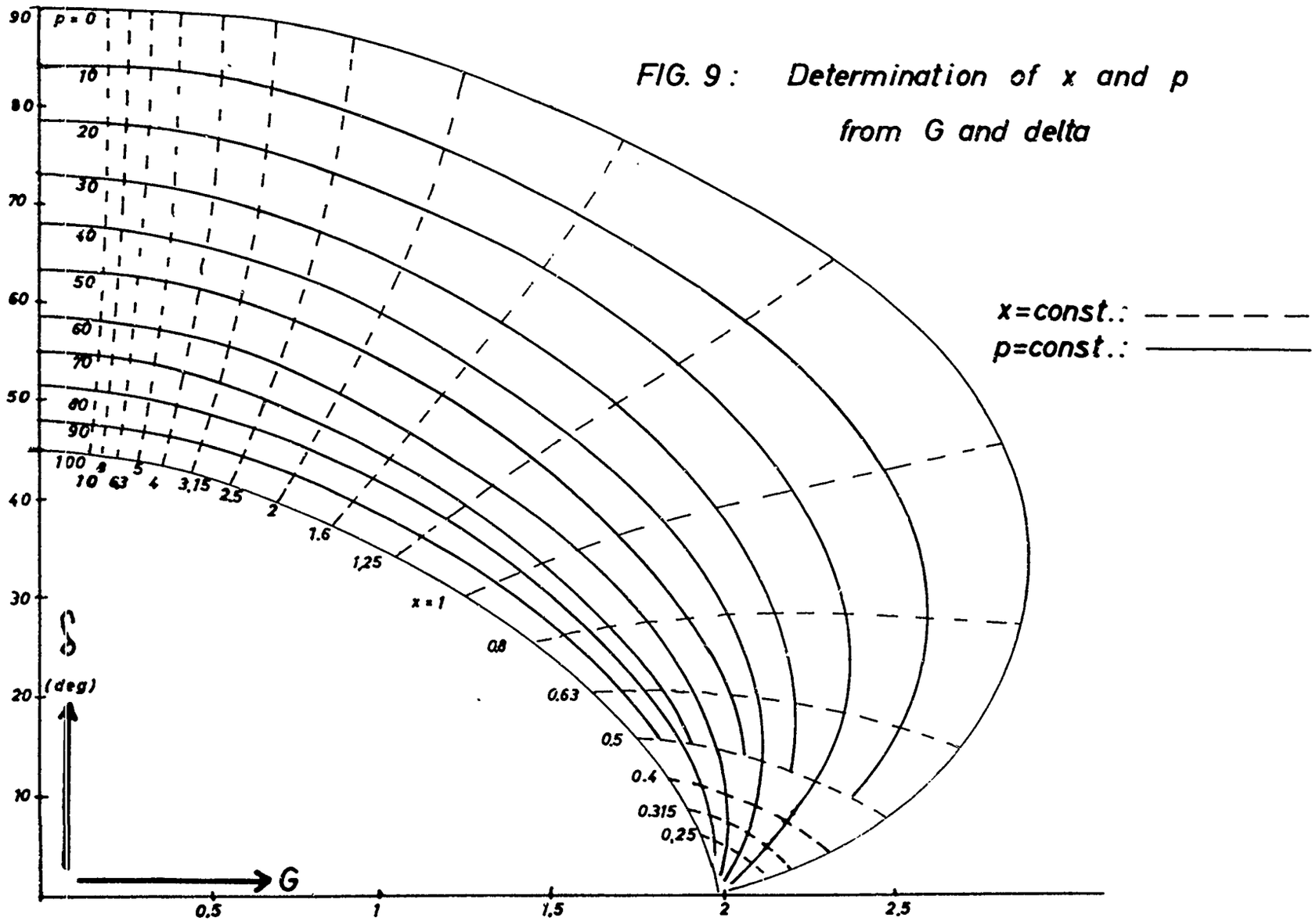

FIG. 9 : Determination of x and p from G and delta

x=const.: — — — — —

p=const.: ————

2. EXPERIMENT

2.1. Transmitter and receiver

All the instruments (transmitter and receiver) described in [3] or [5] could be used for the measurements.

The transmitter consists of the collapsible frame antenna SA 11, built on an automatic antenna rotating device. The latter turns the transmitting antenna with steps of 15 degrees, the transmitter being switched off during the rotation. Thus, the adjustment of a new angular position is indicated on the receiver. SA 11 and the tuning units are connected in series resonance circuit, operated with 120 kc/sec by a battery-fed transmitter.

At the receiver side, a ferrite rod is used as receiving antenna. It is fixed on a bearing head (Fig. 10). The magnetic field variable in time, induces a voltage in a winding with grounded center-tap, fixed symmetrically to the center of the ferrite rod. This voltage is conducted to a tuning and preamplifier unit. From there, the signal goes to a wave analyser having a band width of 100 cps (SFM-2, Wandel & Goltermann).

2.2. Evaluation of measurements (method I)

The condition of homogeneity seems to be largely satisfied in the mine of St. Gertraudi. Several measurements as described in [5] have been evaluated according to 1.9. The axes of the polarisation ellipse and the angularity of the receiving antenna are measured for each angular position of the receiving antenna. Thus, a number of G and δ values are obtained for various values of ϑ. They are averaged and the standard error of the arithmetic mean is determined. From Fig. 9, the deviations of x and p are then calculated from the equations, and finally the standard error of the

arithmetic mean of ε and σ is obtained:

$$\frac{\Delta\varepsilon}{\varepsilon} = \sqrt{2\left[\left(\frac{\Delta x}{x}\right)^2 + \left(\frac{\Delta r}{r}\right)^2 + \left(\frac{\Delta y}{y}\right)^2 + \frac{\Delta p}{\frac{1}{p} - p}\right]} \qquad (29)$$

$$\frac{\Delta\sigma}{\sigma} = \sqrt{2\left(\frac{\Delta x}{x}\right)^2 + 2\left(\frac{\Delta r}{r}\right)^2 + \frac{\Delta p}{p} + \frac{\Delta y}{y}} \quad . \qquad (30)$$

The peculiar term $\frac{\Delta p}{\frac{1}{p} - p}$ in (29) means:

If p approaches unity, the method fails for determining ε. This, however, becomes quite clear: From $p \doteq 1$ it follows that

$$\frac{\sigma}{\omega\varepsilon\varepsilon_o} \gg 1$$

according to Section 1.6. The conduction current thus predominates over the displacement current to such a degree that the quantity ε has but a very small influence on G and δ.
Example: Let

$$\frac{\sigma}{\omega\varepsilon\varepsilon_o} = 20$$

then $$p = 1 - \frac{1}{20} = 0.95,$$

and if σ becomes twice as large, we obtain

$$\frac{\sigma}{\omega\varepsilon\varepsilon_o} = 40$$

and $$p = 1 - \frac{1}{40} = 0.975 \ ,$$

i.e., a 100 per cent change of ε in this region yields a change in p which is not even 3%!

The transmitting antenna and receiving antenna were at first adjusted with respect to the north direction, and the angles of interest were calculated according to the relations (cf. Fig. 1)

$$\vartheta = \vartheta_N - \varphi_N \qquad (31)$$

$$\Psi = \varphi_N - \alpha_N \qquad (32)$$

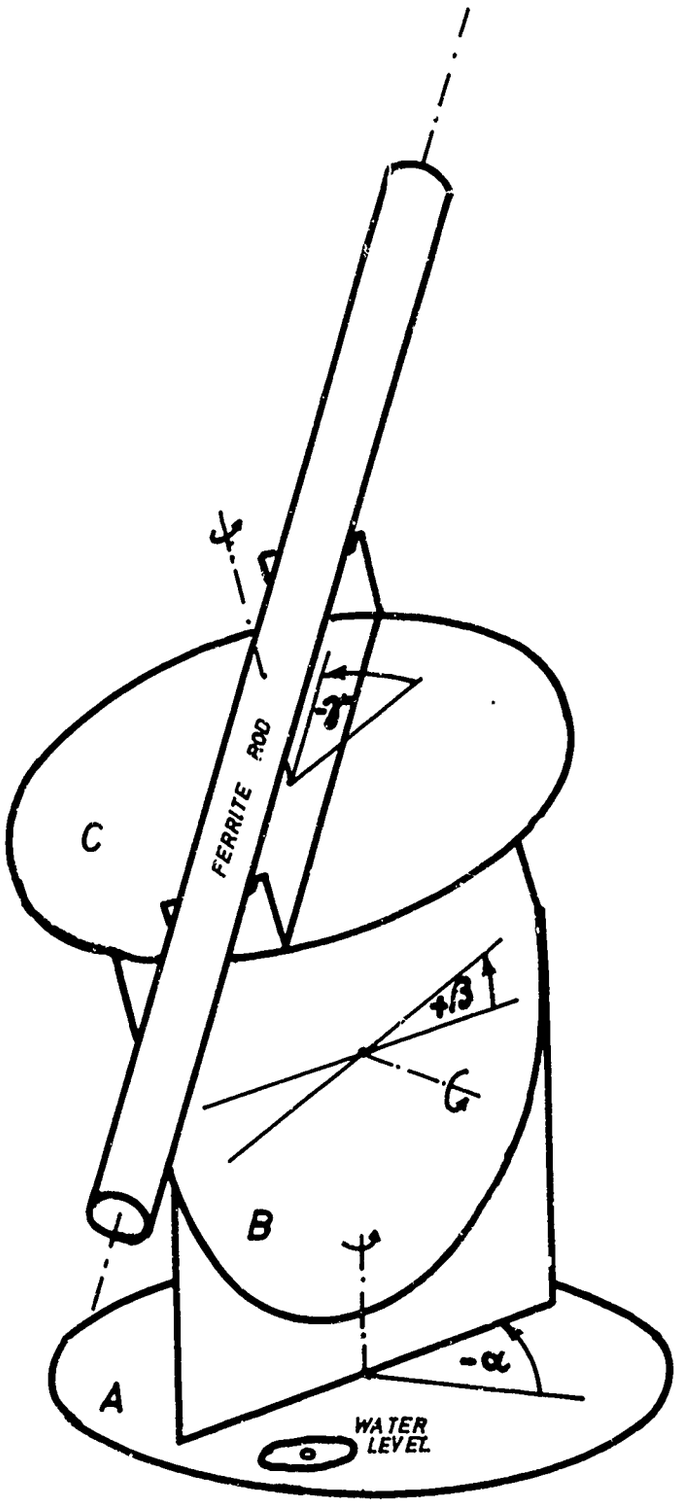

FIG. 10 : Bearing Head for Receiving Antenna

The orientation of angles can also be found in Fig. 1. The angular values of α_N, β, γ were adjusted in accordance with directional method I [5] . Eq. (32) is valid only if the maximum of the polarization ellipse is horizontal. This was the case in the present measurement. Table 1 gives in brief the minutes of the measurement and its evaluation. (The angles γ and β which had not been evaluated, were omitted, as well as the voltage in direction of the absolute minimum, i.e., in direction of the surface normal of the polarization ellipse.)

The point at which transmitter and receiver had been set up can be found in the miner's map (Fig. 11). We obtain

$$\sigma = (1.9 \pm 0.2) \cdot 10^{-4} \text{ mhos/m}$$

$$\varepsilon = 13 \pm 2$$

Tables 2a and 2b contain two measurements in which transmitter and receiver were interchanged. The mean values of G and δ coincide for each measurement separately, thus the mean values of both measurements could be determined jointly. The accuracy was somewhat improved:

$$\sigma = (2.4 \pm 0.2) \cdot 10^{-4} \text{ mhos/m}$$

$$\varepsilon = 10.5 \pm 1 .$$

The errors are always to be understood as standard errors of the arithm. mean. Some lines of the Tab. have not been evaluated. These are either reading errors, mostly, however, they contain δ values near 0° and 90°. Here, one field strength component prevails to such an extent that the evaluation of the polarization ellipse becomes useless owing to the attainable accuracy of angle adjustment.

There exists an additional method of checking the mean values of G: They must coincide with the directly measured voltage ratio

at $\vartheta = 0^\circ$ and $\vartheta = 90^\circ$ according to the definition of G (10). This was the case in the present measurement.

For an accurate control of theory, the position of the polarization ellipse in space must also be evaluated. This plane is given by the surface normal and by the point P of the measurement. The direction of the surface normal, however, is identical with the direction of U_3 (= direction of minimum field strength of reception) which can be adjusted most accurately because of the cosine characteristics of the receiving antenna.

In the directional method I [5] , the direction of U_3 is fixed by three angles. An arbitrary spatial direction, however, can be adjusted with two angles, as applied in method II. Hence, method II seems to be more suited for evaluating the position of the polarization ellipse in space.

2.3. Measurements by directional method II

Tables 3a and 3b contain two measurements in which transmitter and receiver were again interchanged. If U_1 is horizontal, we have $\gamma \approx 0$, yielding

$$\psi - \alpha = \pm 90^\circ \qquad (33)$$

(both signs , because ψ can be determined only to $\pm 180^\circ$).
α is obtained from

$$\alpha = \vartheta_N - \alpha_N \ . \qquad (34)$$

Evaluation yielded

$$\sigma = (1.5 \pm 0.2) \cdot 10^{-4} \text{ mhos/m}$$
$$\varepsilon = 7.5 \pm 1 \ .$$

These measurements, however, show that the polarization ellipse does not lie in the horizontal plane as could be expected from theory. An increase in gallery height is not sufficient for ex-

FIG. 11: Mine of St. Gertraudi (Großkogel)

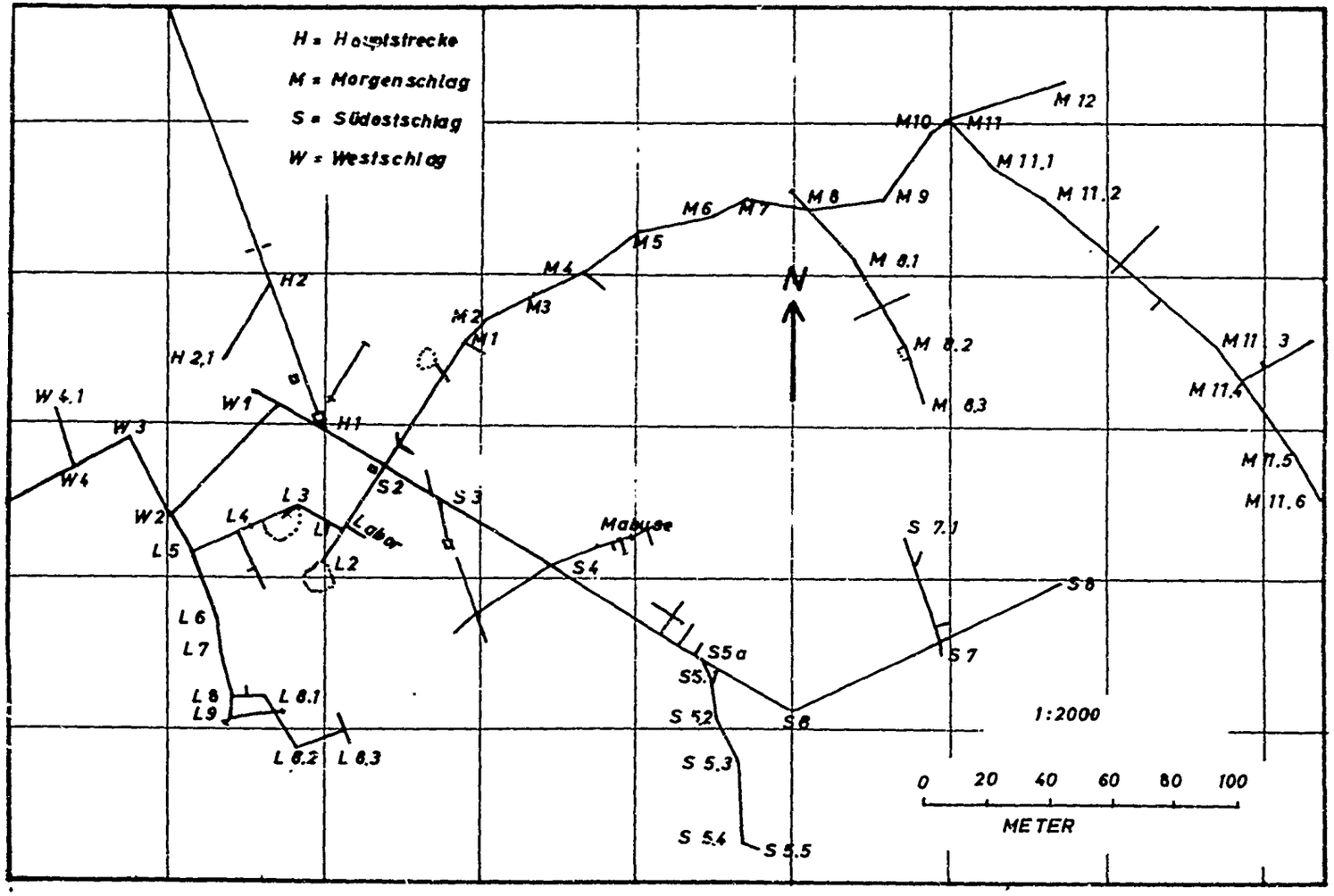

plaining the deviation of ß from 90°. The number of measurements is too small as to permit any conclusions regarding the causes why the plane of the measured polarization ellipse deviates from the meridional plane.

If this deviation is neglected in first approximation, this method of determining σ and ε is well permitted. More so, if the resulting values agree with those obtained from a completely different method.

2.4. Comparison

σ and ε of rock samples were determined in [6] with a measuring capacitor by a bridge method. The rock occurring most frequently in St. Gertraudi yielded the following values:

	ε	σ(mhos/m)
white dolomite	12.8	$1.2 \cdot 10^{-4}$
yellow dolomite	13	$2 \cdot 10^{-4}$
sandstone	5.5	$6 \cdot 10^{-4}$
water	81	$4.3 \cdot 10^{-2}$

The values obtained from the propagation measurements are in fairly good agreement with those of the natural samples.

Summary

In the theoretical part, the possibility of determining σ and ε from the field structure of the magnetic dipole was shown. Decisive for the field structure is the complex propagation constant besides the distance r. The field can be characterized not only by k_1, k_2 and r, but also by G, the ratio of the receiving field strength at $\vartheta = 0^{\circ}$ and 90°, and by the phase difference δ between the field strength components H_r and H_ϑ. G and δ can be determined by evaluating the polarization

ellipse, thus δ and ε are obtained.

In the experimental part, some measurements have been described and the agreement of δ and ε with those of the natural samples has been illustrated. The deviations of theory and experiment observed in a declination of the plane of the measured polarization ellipse toward the meridional plane shall be the subject of further studies.

MEASUREMENTS IN ST. GERTRAUDI

with the portable transmitter.

Frequency: 120 kc/sec.

TABLE 1

27 April 1966

Transmitter: End of "Südostschlag"

Receiver: Bend of "

Distance r = 92 m

Angle from north towards r : φ_N = 242 deg.

φ_N	α_N	[mV] U_1	[mV] U_2	$\frac{U_1}{U_2}$ v	ψ	φ	cot φ	$\frac{A}{B}$ w	δ	G
180	298	230	60	3.8	-56	-62	0.532	0.71	31.5	1.34
165	317	255	20	12.8	-75	-77	0.231	0.24		
150	335	225	21	10.7	-87	+88				
135	353	235	66	3.6	69	73	0.306	0.48	42	1.57
120	14	259	95	2.7	48	58	0.625	0.92	39.5	1.47
105	32	270	95	2.8	30	43	1.07	1.51	42	1.41
90	45	300	81	3.7	17	28	1.88	2.35	44	1.25
75	54	320	52	6.15	8	13	4.33	4.5	47	-
60	64	320	17	19	- 2	- 2				
45	73	305	19	16	-10	-17	3.27	2.85		
30	83	280	48	5.85	-21	-32	1.60	2.4	27.5	1.50
15	97	260	67	3.9	-35	-47	0.933	1.38	31	1.59
0	117	235	62	3.8	-55	-62	0.532	0.71	31.5	1.34

$\bar{G} = 1.43 \pm 0.04$
$\bar{\delta} = 37.5 \pm 3$
$\Longrightarrow$ $x = 1.06 \pm 0.06$, $p = 0.68 \pm 0.08$ $\Longrightarrow$

$\Longrightarrow$ $\sigma = (1.9 \pm 0.2).10^{-4}$ mhos/m
$\varepsilon = 13 \pm 2$

TABLE 2

22 March 1966 , 29 March 1966

a) Transmitter: Morgenschlag-Süd VI

Receiver: Bend of Südostschlag

b) same as a), but transmitter and receiver interchanged

r = 178 m, $\vartheta_N = 35^\circ$ ($\pm 180^\circ$)

	ϑ_N	α_N	U_1	U_2	v	Ψ	ϑ	tanϑ	w	δ	G
a)	360	261									
	345	278	41	17	2.4	-63	-50	1.19	0.63	51.5	0.75
	330	289	37	10	3.7	-74	-65	2.14	0.43	48	0.92
	315	298	38	6	6.3	-83	-80	5.67	0.20	48	
	300	305	41	3.2	12.8	90	85	11.45			
	285	315	40	6.2	6.45	80	70	2.58	0.24	42	0.62
	270	327	37	10	3.7	68	55	1.43	0.40	39.5	0.56
	255	348	34	11	3.1	47	40	0.84	0.95	35.5	0.80
	240	2	32	6	5.3	33	25	0.467	1.68		0.79
	225	22	32	2.5	12.8	13	10	0.176	4.0		0.70
	210	38	38	8	4.8	- 3	- 5	0.08			
	195	55	34	14	2.43	-28	-20	0.364	1.28	49.5	
	180	83	33	16	2.06	47	-35	0.700	0.985	52.5	0.69
b)	360	252	47	24	2.0	-45	-35	0.700	1.0	53	0.70
	345	276	53	25	2.15	-61	-50	1.19	0.71	55	0.85
	330	292	9	21	2.8	-77	-65	2.14	0.485	55	
	315	303	63	14	4.5	-89	-80	5.67	0.24		
	300	310	65	6.5	10.0	85	85	11.45	7.5	49	
	285	318	63	6	10.5	77	70	2.58	0.26		0.67
	270	328	59	12	4.9	67	55	1.43	0.58	30.5	0.83
	255	342	52	16	3.25	53	40	0.84	0.84	35.5	0.71
	240	2	48	16	3.0	33	25	0.467	1.64	39	0.77
	225	24	46	10	4.6	11	10	0.176	3.5	52	0.62
	210	39	46	7	6.6	- 4	- 5	0.08	6.0	63	
	195	56	47	16	2.94	-21	-20	0.364	1.94	46.5	0.71
	180	80	48	24	2.0	-45	-35	0.700	1.0	53	0.70

$\bar{G} = 0.73 \pm 0.02$
$\bar{\delta} = 47 \pm 1.6$
$\rightarrow$ $x = 2.2 \pm 0.1$, $p = 76 \pm 6\ \%$ $\rightarrow$

$\rightarrow$ $\sigma = (2.4 \pm 0.2).10^{-4}$ mhos/m

$\varepsilon = 10.5 \pm 1$

TABLE 3

10 May 1967

a) Transmitter: Bend of Südostschlag

Receiver: At point 8.2, Morgenschlag-Süd I

r = 122 m , φ_N = 14° (± 180°)

b) same as a)m but transmitter and receiver interchanged.

φ_N	U_1	U_2	α_N	B	γ	v	α	Ψ	δ	tan δ	w	δ	G
0	146	26	298	-67	1	5.6	76	-14	-14	0.25	3.3	35	0.825
15	147	12	288	-29	0	12.2	84	- 6	1	-	7.5	40	-
30	145	16.5	98	-51	-1	8.9	-84	6	16	0.285	6.5	48	1.86
45	140	30	85	-69	1	4.2	-71	19	31	0.601	2.4	40	1.44
60	125	38	72	-75	-7	3.3	-58	32	46	1.035	1.5	36	1.56
75	122	35	54	-76	-6	3.5	-40	50	61	1.805	0.86	32	1.55
90	120	19	35	-73	-1	6.3	21	69	76	2.6	0.39	-	1.02
105	125	32	20	-90	0	3.9	- 6	-84	91	-	0.32	-	-
120	125	26	1	-90	0	4.8	-14	-76	-74	4.0	0.33	42	1.32
135	-	-	-	-	-	-	-	-	-59	-	-	-	-
150	125	42	328	-84	8	3.0	46	-44	-44	0.966	1.02	35	0.89
165	140	37	317	-80	11	3.8	57	-23	-29	0.555	2.0	34	1.11
180	-	-	299	-63	2	-	75	-15	-14	0.25	-	-	-
360													
345	85	26	319	90	0	3.3	55	-25	-29	0.555	1.55	37	0.86
330	85	32	326	82	1	2.65	48	-32	-44	0.966	1.45	45	1.40
315	85	27	341	81	1	3.0	33	-57	-59	1.065	0.71	38	1.18
300	80	16	358	7.5	4	5.0	12	-78	-74	3.5	0.29	42	1.01
285	-	-	20	- 5	-	-	34	-	91	-	-	-	-
270	85	16	69	96	-35	5.3	83	43	76	-	-	-	-
255	85	24	50	90	0	3.5	-36	54	61	1.805	0.77	33	1.39
240	95	24	71	90	0	4.0	-57	33	46	1.035	1.45	30	1.51
225	100	17.5	264	90	0	5.7	-70	20	31	0.601	2.95	29	1.77
210	103	2	285	-67	0	50	89	- 1	16	0.287	3	-	-
195	103	7	286	60	0	19.7	88	- 2	1	-	-	-	-
180	100	18	298	76	-4	5.55	76	-14	-14	0.25	3.3	35	0.825

$\bar{G}$ = 1.25 ± 0.08
$\bar{\delta}$ = 37 ± 1.2° } → x = 1.18 ± 0.1, p = 77 ± 10 % } → $\sigma = (1.5 \pm 0.2) \cdot 10^{-4}$ mhos/m, ε = 7.5 ± 1

LIST OF ILLUSTRATIONS

REFERENCES

[1] Electro-Technology Nr. 61, Jan. 1964
Charles L. Marquardt: The Near Electromagnetic Field.

[2] 2nd Technical Annual Summary Report: On the propagation of VLF waves in solids, 61(052)-490, Dec. 1962

[3] Jahresbericht 1966 des VLF-Forschungsprojektes Contract 61(052)-902

[4] Dokupil S.-Karpinsky I. The attenuation of Electromagnetic Waves in Rock. Studia geoph. et geod. 6, 176-192,1962

[5] Scientific Report No. 2, 1967, Contract Nr. 61(052)-902
N. Nessler: Propagation of long electromagnetic waves through rock

[6] Scientific Report Nr. 3 1967, Contract Nr. 61(052)-902
H. Wöbking: The Frequency Dependence of the Dielectric Constant and Conductivity of Rock and its Relation to Quantities of Rock Fabric.

[7] K. Fränz und H. Lassen: Antennen und Ausbreitung 2. Auflage, Springer Verlag/Berlin 1956

[8] G. Joos: Lehrbuch der theoret. Physik 11. Aufl. Akad. Verlagsgesellschaft Geest u. Portig KG. Leipzig 1964

[9] J.A. Stratton: Electromagnetic Theory
McGraw Hill Book Co. Inc., New York 1941

DOCUMENT CONTROL DATA - R&D

1. ORIGINATING ACTIVITY (Corporate author)
Dr. Wolfram BITTERLICH
Kaiser-Franz-Josefstr. 5
A-6020 Innsbruck, Austria

2a.

2b. GROUP

3. REPORT TITLE
DETERMINATION OF THE MEAN VALUES OF CONDUCTIVITY AND DIELECTRIC CONSTANT FROM THE FIELD STRUCTURE OF A MAGNETIC DIPOLE

4. DESCRIPTIVE NOTES (Type of report and inclusive dates)
SCIENTIFIC REPORT NO. 4

5. AUTHOR(S) (Last name, first name, initial)
Walter KELLNER

6. REPORT DATE	7a. TOTAL NO. OF PAGES	7b. NO. OF REFS
20 June 1967	36	9

8a. CONTRACT OR GRANT NO.
CONTRACT AF 61(052)-902
b. PROJECT AND TASK NO.
4600-11
c. ELEMENT
62405454
d. SUBELEMENT
674600

9a. ORIGINATOR'S REPORT NUMBER(S)

9b. OTHER REPORT NO(S) (Any other numbers that may be assigned this report)

10. DISTRIBUTION STATEMENT
DISTRIBUTION OF THIS DOCUMENT IS UNLIMITED

11. SUPPLEMENTARY NOTES

12. SPONSORING ACTIVITY
United States Government
American Embassy, Brussels, Belgium

13. ABSTRACT

The equations for a magnetic dipole in a homogeneous, conductive medium are analyzed. The field is shown to be elliptically polarized in the transition zone between near field and far field. Quantities are introduced which are easy to determine by experiment: from them, the complex propagation constant can be determined at a given distance. Thus, conductivity and dielectric constant can be calculated for a given frequency. The applicability of this method is confined to the region of validity of the basic expressions. This comprises the condition that the cavity which contains transmitter and receiver is small as compared to the wave-length in matter. Our measurements at 120 kc/sec satisfied this condition.

The principle of measurement and its evaluation are described. The results are compared with results obtained from natural rock samples.

1473

14. KEY WORDS	LINK A		LINK B		LINK C	
	ROLE	WT	ROLE	WT	ROLE	WT
Complex propagation constant Field structure of a magnetic dipole Transition zone between near field and far field Phase shift Polarization ellipse Determination of σ and ε						